

Chemical reaction and radiation effects on dissipative MHD stagnation point flow of Casson nanofluid over a non linear stretching sheet with velocity slip and convective boundary conditions

¹Srinivasasai panuganti, ²RameshMudda ³M.S.Sudhir, ⁴PadmaPolarapu

¹Department of mathematics,S.S.&N.College,Narasaraopet-522601,A.P.

²Department of mathematics,S.S.&N.College,Narasaraopet-522601,A.P.

³Department of chemistry,S.S.&N.College,Narasaraopet-522601,A.P.

⁴Department of mathematics,GovernmentDegreeCollege,Yellandu ,Telangana

Email: p.srinivasasai@gmail.com,

Abstract

The current paper deals with the magnetohydrodynamic (MHD) stagnation point flow of Casson nanofluid over a nonlinear stretching sheet in the presence of velocity slip and convective boundary condition. In this analysis, various effects such as velocity ratio, viscous dissipation and chemical reaction have been accentuated. Possessions of Brownian motion and thermophoresis are also depicted in this study. A uniform magnetic field as well as suction is taken into account. Suitable similarity transformations are availed to convert the governing nonlinear partial differential equations into a system of nonlinear ordinary differential equations and then solving the system of equations by using Runge–Kutta–Fehlberg fourth–fifth order method, notable accuracy of the present results has been obtained with the earlier results. Impact of distinct parameters on velocity, temperature, concentration, skin friction coefficient, Nusselt number and Sherwood number is canvassed through graphs and tabular forms.

Keywords: Casson nanofluid, stagnation point flow, suction, slip boundary condition, convective boundary condition.

Nomenclature

| | |
|---------------------------------|---|
| u, v | velocity components in x and y directions |
| k | thermal conductivity |
| $\alpha = \frac{k}{(\rho c)_f}$ | thermal diffusivity |
| σ | electrical conductivity |
| B_0 | Constant |
| ν | kinematic viscosity |
| β | Casson fluid parameter |
| ρ_f | density of the base fluid |
| D_B | Brownian diffusion coefficient |
| D_T | thermophoresis diffusion coefficient |
| Q_0 | volumetric heat generation/absorption |
| C_p | specific heat at constant pressure |
| T | fluid temperature |
| C | fluid concentration |
| k_0 | chemical reaction coefficient |
| v_w | velocity of suction |
| ψ | stream function |
| T_w | wall temperature |
| C_w | nanoparticle concentration |
| T_∞ | ambient value of temperature |
| C_∞ | ambient value of the nanoparticle fraction |
| $(\rho c)_f$ | heat capacity of the fluid |

| | |
|---|---|
| $(\rho c)_p$ | effective heat capacity of a nanoparticle |
| n | nonlinear stretching parameter |
| a, b | positive constants |
| $U_w = ax^n$ | stretching velocity |
| $U_\infty = bx^n$ | free stream velocity |
| $U_{slip} = \left(\mu_B + \frac{p_y}{\sqrt{2\pi_c}} \right) \frac{\partial u}{\partial y}$ | slip velocity |
| $B(x)$ | magnetic field |
| $A = \frac{b}{a}$ | velocity ratio parameter |
| $\delta = \mu_B \sqrt{\frac{a(n+1)}{2\nu}} x^{\frac{n-1}{2}}$ | slip parameter |
| $Bi = \frac{h_f}{k} \sqrt{\left(\frac{2\nu}{a(n+1)} \right)} \frac{1}{x^{\frac{n-1}{2}}}$ | Biot number |
| $M = \frac{2\sigma B_0^2}{a\rho_f(n+1)}$ | magnetic parameter |
| $Pr = \frac{\nu}{\alpha}$ | Prandtl number |
| $R = \frac{4\sigma^* T_\infty^3}{k^* k}$ | radiation parameter |
| $Nb = \frac{(\rho c)_p D_B (C_w - C_\infty)}{\nu (\rho c)_f}$ | Brownian motion parameter |
| $Nt = \frac{(\rho c)_p D_T (T_f - T_\infty)}{\nu (\rho c)_f T_\infty}$ | thermophoresis parameter |
| $Ec = \frac{U_w^2}{C_p (T_f - T_\infty)}$ | Eckert number |

$$Le = \frac{\nu}{D_B} \quad \text{Lewis number}$$

$$\gamma = \frac{2\nu x k_0}{(n+1)U_w} \quad \text{chemical reaction parameter}$$

$$S = -\frac{v_w}{\sqrt{\frac{a\nu(n+1)}{2}x^{\left(\frac{n-1}{2}\right)}}} \quad \text{suction parameter}$$

Subscripts

w condition at the surface
 ∞ condition at the free stream

1.Introduction

In nature, non-Newtonian fluid acts as an elastic solid i.e. the flow does not occur with small shear stress. Casson fluid is one of the non-Newtonian fluids. It was first invented by Casson in 1959. It is based on the structure of liquid phase and interactive behaviour of solids of a two-phase suspension. Some examples of Casson fluid are jelly, honey, tomato sauce and concentrated fruit juices. Human blood can also be treated as a Casson fluid in the presence of several substances such as fibrinogen, globulin in an aqueous base plasma, protein and human red blood cells.

Nanofluid is a new type of fluid proposed by Choi [1] at the time of investigations on coolants techniques and cooling processes. These fluids are creating a great deal of interest due to their tremendous potential with respect to enhanced heat transfer. The effect of Brownian motion and thermophoresis in nanofluid was first considered by Buongiorno [2]. By using this model, Khan and Pop [3] studied the boundary layer flow of a nanofluid over a stretching sheet. Mustafa et al. [4], Ibrahim et al. [5], Bachok et al. [6] and others have analysed the stagnation point flow of nanofluids. Yacob et al. [7] and Makinde and Aziz [8] have also reported problems on nanofluid flow over a stretching sheet by taking convective boundary condition at the surface.

Magnetic nanofluid is a colloidal suspension of carrier liquid and magnetic nanoparticles. MHD was first tested in geophysical and astrophysical problems. In recent years, MHD has received

significant attention owing to its various applications in engineering and petroleum industries. Magnetic nanofluid is also one of them and the main objective of this research area is that fluid flow and transfer of heat can be controlled by external magnetic field. The effect of magnetic field on nanofluid with different geometries has been investigated by several researchers. . Influence of thermal radiation on the flow of natural convection boundary layer of a nanofluid past a vertical plate with uniform heat flux has been studied by Gnanaswara Reddy[9]. Thermal radiation effects on MHD stagnation point flow of a nanofluid over a stretching sheet in a porous medium have been reported very recently by Gnanaswara Reddy et al.[10]. Sathies kumar and Gangadhar[11] proposed the effect of chemical reaction on slip flow of MHD Casson fluid over a stretching sheet under the influence of heat and mass transfer. Bhattacharyya [12] examined the thermal radiation effect on MHD stagnation point flow of Casson fluid over a stretching sheet. Unsteady magnetohydrodynamic Casson fluid flow over a vertical cone and flat plate in presence of non-uniform heat source was explained by Benazir et al. [13].

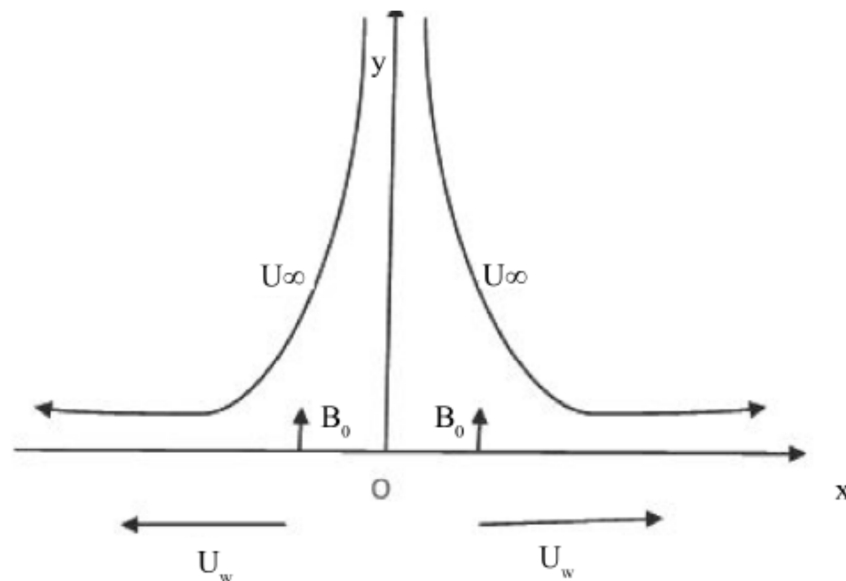
Nadeem et al. [14] proposed the MHD 3D Casson fluid flow past a porous linearly stretching sheet. Convective heat transfer and MHD effects on Casson nanofluid over a shrinking sheet were described by Rizwan et al [15]. Ibrahim and Makinde [16] developed the MHD stagnation point flow and heat transfer of Casson nanofluid past a stretching sheet under the influence of velocity slip and convective boundary conditions. The effects of heat and mass transfer on MHD flow of Casson fluid under the influence of chemical reaction with suction was carried out by Shehzadl et al.[17]. Mukhopadhyay [18] derived the importance of thermal radiation on Casson fluid flow with heat transfer over a stretching surface in presence of suction and injection. The Casson nanofluid over a stretching sheet in presence of thermal radiation, convective and velocity slip boundary conditions was illustrated by Oyelakin et al. [19].

All the above investigations are restricted to the flow over a linearly stretching sheet but it is not necessary that the stretching sheet has to be linear. Casson fluid flow and heat transfer over a nonlinearly stretching surface was formulated by Mukhopadhyay [20]. Vajravelu [21] analyzed the viscous flow over a nonlinearly stretching sheet. The heat transfer characteristics of a viscous fluid over a non linear stretching sheet were later introduced by Cortell [22]. Pal et al. [23] briefed the effects of thermal radiation on MHD Casson nanofluid flow over a vertical non-linear stretching surface in presence of Joule heating by using the scaling group method. Ullah et al.

[24] studied MHD mixed convection slip flow of Casson fluid over a nonlinearly stretching sheet embedded in a porous medium in presence of chemical reaction, thermal radiation, heat generation and convective boundary conditions. Chemical reaction and heat source effects on mixed convection flow of Casson nanofluid over a stretching sheet in presence of convective boundary conditions was derived by Hayat et al. [25]. The flow and diffusion of chemically reactive species over a nonlinearly stretching sheet immersed in a porous medium have been explored by Ziabakhsh et al. [26]. A great number of studies for the boundary layer flow over a non linear stretching sheet with different aspects of heat and mass transfer, slip and convective boundary conditions etc., are presented in the literature [27]-[37].

In the current paper, investigation has been made to study the MHD stagnation point flow of a Casson nanofluid over a nonlinear stretching sheet in the presence of velocity ratio, suction, thermal radiation, viscous dissipation, chemical reaction, Brownian motion, thermophoresis, slip and convective boundary conditions. The flow, heat and mass transfer equations are solved by using Runge–Kutta–Fehlberg fourth–fifth order method

2.Mathematical formulation



Consider a steady two-dimensional dissipative MHD stagnation point flow of an incompressible Casson nanofluid over a nonlinear stretching sheet which coincides with the plane $y = 0$. The flow being confined to the region $y \geq 0$, it is assumed that $u = U_w = ax^n$ is the stretching velocity of the sheet and $U_\infty = bx^n$ is the free stream velocity where $a > 0$, $b > 0$ are constants, and $n \geq 0$ is the nonlinear stretching parameter. The slip velocity at the surface is taken as $U_{slip} = \left(\mu_B + \frac{p_y}{\sqrt{2\pi_c}} \right) \frac{\partial u}{\partial y}$. The temperature of the sheet is regulated by a convective heating process which is symbolised by a temperature T_f and a heat transfer coefficient h_f . It is assumed that C_w is the nanoparticle concentration and as $y \rightarrow \infty$, the ambient values of temperature and nanoparticle concentration are T_∞ and C_∞ . A magnetic field $B(x) = B_0 x^{\frac{n-1}{2}}$ is applied perpendicularly to the sheet with constant B_0 . The rheological equation of state for an isotropic and incompressible flow of Casson fluid is

$$\tau_{ij} = \begin{cases} 2 \left(\mu_B + \frac{p_y}{\sqrt{2\pi}} \right) e_{ij}, & \pi > \pi_c \\ 2 \left(\mu_B + \frac{p_y}{\sqrt{2\pi_c}} \right) e_{ij}, & \pi_c > \pi \end{cases}$$

where μ_B is the plastic dynamic viscosity of the fluid which is non-Newtonian, p_y is the yield stress of the fluid, π is the product of the component of deformation rate with itself, $\pi = e_{ij}e_{ij}$, e_{ij} is the $(i, j)^{th}$ component of the deformation rate and π_c is the critical value of this product based on the non-Newtonian model.

Under these assumptions, the equations governing the flow can be written as

$$\frac{\partial u}{\partial x} + \frac{\partial v}{\partial y} = 0, \quad (1)$$

$$u \frac{\partial u}{\partial x} + v \frac{\partial u}{\partial y} = v \left(1 + \frac{1}{\beta} \right) \frac{\partial^2 u}{\partial y^2} + U_\infty \frac{\partial U_\infty}{\partial x} + \frac{\sigma B^2(x)}{\rho_f} (U_\infty - u), \tag{2}$$

$$u \frac{\partial T}{\partial x} + v \frac{\partial T}{\partial y} = \alpha \frac{\partial^2 T}{\partial y^2} + \frac{(\rho c)_p}{(\rho c)_f} \left[D_B \frac{\partial C}{\partial y} \frac{\partial T}{\partial y} + \frac{D_T}{T_\infty} \left(\frac{\partial T}{\partial y} \right)^2 \right] + \frac{v}{C_p} \left(1 + \frac{1}{\beta} \right) \left(\frac{\partial u}{\partial y} \right)^2 - \frac{1}{(\rho c)_f} \frac{\partial q_r}{\partial y} \tag{3}$$

$$u \frac{\partial C}{\partial x} + v \frac{\partial C}{\partial y} = D_B \frac{\partial^2 C}{\partial y^2} + \frac{D_T}{T_\infty} \frac{\partial^2 T}{\partial y^2} - k_0 (C - C_\infty). \tag{4}$$

Subject to the boundary conditions

$$u = U_w + U_{slip} = a x^n + \left(\mu_B + \frac{p_y}{\sqrt{2\pi_c}} \right) \frac{\partial u}{\partial y}, v = v_w, -k \frac{\partial T}{\partial y} = h_f (T_f - T), C = C_w \text{ at } y = 0, \tag{5}$$

$$u \rightarrow U_\infty = b x^n, v \rightarrow 0, T \rightarrow T_\infty, C \rightarrow C_\infty \text{ as } y \rightarrow \infty.$$

Now, we introduce the following similarity transformations in order to convert the partial differential equations into ordinary differential equations:

$$\left. \begin{aligned} u &= a x^n f'(\xi), \xi = y \sqrt{\frac{a(n+1)}{2\nu}} x^{\frac{(n-1)}{2}}, v = -\sqrt{\frac{a\nu(n+1)}{2}} x^{\frac{(n-1)}{2}} \left(f(\xi) + \frac{n-1}{n+1} \xi f'(\xi) \right), \\ \psi &= \sqrt{\frac{2a\nu}{(n+1)}} x^{\frac{(n+1)}{2}} f(\xi), \theta(\xi) = \frac{T - T_\infty}{T_f - T_\infty}, \phi(\xi) = \frac{C - C_\infty}{C_w - C_\infty}, \end{aligned} \right\} \tag{6}$$

where ξ is the similarity variable, ψ is the stream function.

The stream function ψ is formalized in the standard way as

$$u = \frac{\partial \psi}{\partial y}, \quad v = -\frac{\partial \psi}{\partial x}.$$

Here we assume $v_w = -\sqrt{\frac{a\nu(n+1)}{2}} x^{\frac{(n-1)}{2}} S$, where S is the suction parameter.

Substituting Equation (6) in Equations (2) to (5), we obtain

$$\left(1 + \frac{1}{\beta} \right) f'''' + f f'' - \frac{2n}{n+1} (f'^2 - A^2) + M(A - f') = 0, \tag{7}$$

$$\left(1 + \frac{4}{3}R\right)\theta'' + \text{Pr} f \theta' + \text{Pr} Nb \theta' \phi' + \text{Pr} Nt \theta'^2 + \left(1 + \frac{1}{\beta}\right) \text{Pr} Ec f'^2 = 0, \quad (8)$$

$$\phi'' + Le f \phi' + \frac{Nt}{Nb} \theta'' - Le \gamma \phi = 0. \quad (9)$$

The boundary conditions are

$$\begin{aligned} f(0) = S, \quad f'(0) = 1 + \delta \left(1 + \frac{1}{\beta}\right) f''(0), \quad \theta'(0) = -Bi(1 - \theta(0)), \quad \phi(0) = 1, \\ f'(\infty) \rightarrow A, \quad \theta(\infty) \rightarrow 0, \quad \phi(\infty) \rightarrow 0, \end{aligned} \quad (10)$$

where prime denotes differentiation with respect to ξ .

Non-dimensional skin friction coefficient C_f , local Nusselt number Nu_x and local Sherwood number Sh_x are

$$C_f = \frac{\tau_w}{\rho U_w^2}, \text{ where } \tau_w = \mu_B \left(1 + \frac{1}{\beta}\right) \left(\frac{\partial u}{\partial y}\right)_{y=0}, \quad Nu_x = \frac{xq_w}{k(T_f - T_\infty)} \text{ and}$$

$$Sh_x = \frac{xq_m}{D_B(C_w - C_\infty)},$$

where τ_w is the wall shear stress, q_w and q_m are the heat and mass fluxes at the surface which are defined as:

$$q_w = -\left(k + \frac{16\sigma^* T_\infty^3}{3k^*}\right) \left(\frac{\partial T}{\partial y}\right)_{y=0}, \quad q_m = -D_B \left(\frac{\partial C}{\partial y}\right)_{y=0}.$$

Substituting q_w and q_m in the preceding equations, we get

$$Re_x^{1/2} C_f \sqrt{\frac{2}{n+1}} = \left(1 + \frac{1}{\beta}\right) f''(0), \quad Re_x^{-1/2} Nu_x \sqrt{\frac{2}{n+1}} = -\left(1 + \frac{4}{3}R\right) \theta'(0) \quad \text{and}$$

$$Re_x^{-1/2} Sh_x \sqrt{\frac{2}{n+1}} = -\phi'(0)$$

where $Re_x = \frac{U_w x}{\nu}$ is the local Reynolds number.

3.Method of solution:

The non-linear ordinary differential equations (7) – (9) with boundary conditions (10) are solved using the Runge–Kutta–Fehlberg fourth–fifth order method along with shooting technique. A set of non-linear ordinary differential equations are of third order in f , second order in g , θ and ϕ , and are first reduced into a system of simultaneous ordinary equations. To solve this system by using Runge–Kutta–Fehlberg fourth–fifth order method, one should require three more missed initial conditions. However, the values of $f'(\eta)$, $\theta(\eta)$, $\phi(\eta)$ are known when $\eta \rightarrow \infty$. These end conditions are used to obtain unknown initial conditions at $\eta = 0$ by using shooting technique. In shooting method, the boundary value problem is reduced to that of initial value by assuming initial values. The boundary values calculated have to be matched with the real boundary values. Using trial and error or some scientific method, A scientist attempts to get as close to the boundary value as is possible. The most essential step of this method is to choose the appropriate finite value for far field boundary condition. We took infinity condition at a large but finite value of η where no considerable variations in velocity, temperature and so on occur. We run our bulk computations with the value at $\eta_{\max} = 6.0$, and it is sufficient to achieve the far field boundary conditions asymptotically for all values of the parameters considered.

4.Results and Discussion

This section highlights the influence of arising parameters such as magnetic parameter (M), nonlinear parameter (n), velocity ratio parameter (A), Casson fluid parameter (β), slip parameter (δ), suction parameter (S), Prandtl number (Pr), thermal radiation (R), viscous dissipation (Ec), Brownian motion parameter (Nb), thermophoresis parameter (Nt), Biot number (Bi), Lewis number (Le) and chemical reaction parameter (γ) on velocity, temperature and concentration. Numerical solutions are carried out through Runge–Kutta–Fehlberg fourth–fifth method. For numerical results we considered $\beta = 0.5, M = 0.5, n = 1.5, S = 0.5, A = 0.2,$

$\delta = 0.1, Pr = 0.71, R = 0.1, Nb = 0.1, Nt = 0.1, Ec = 0.1, Bi_1 = 0.5, Le = 2.0$ and $\gamma = 0.5$. These values are conserved as common unless specifically pointed out in the appropriate graphs and tables.

Figs. 1(a) – 1(c) reveal the velocity, temperature and concentration distribution for various values of Casson fluid parameter β . It is noticed that for increasing values of β , the velocity and the boundary layer thickness decrease and increase the temperature and concentration distribution. But here the concentration of the fluid is not being much significant with increase of Casson fluid parameter β .

Figs. 2(a) – 2(c) explain the effect of nonlinear parameter n on velocity, temperature and concentration profiles. It is found that the velocity profile decreases but temperature and concentration profile increases for increasing values of nonlinear parameter. Fig. 3 describes the possession of magnetic parameter M on velocity distribution. The velocity distribution decreases with the magnetic parameter M . This is due to the Lorentz force created by the magnetic field.

Fig. 4 depicts the influence of suction parameter S on velocity profiles. The velocity distributions decelerate with the increase of S . Fig. 5 illustrates the effect of velocity ratio parameter A on velocity field. It is noticed that the velocity increases with A . An increase in the velocity slip parameter δ causes deceleration in nanofluid velocity of the nanofluid. This result is depicted in Fig. 6. An increase in Prandtl number Pr causes an increase in fluid viscosity which causes reduction in temperature. This is shown in Fig. 7.

The effect of radiation parameter R on temperature is displayed in Fig. 8. It is noticed that the temperature rises with the increase of R . The influence of Eckert number Ec on temperature is presented in Fig. 11. As Ec increases the wall temperature also increases due to heat addition by frictional heating. Fig. 10(a) and Fig. 10(b) describe the possession of Brownian motion parameter Nb on temperature and concentration profiles. Temperature enhances with the Brownian motion parameter Nb and the opposite phenomenon is noted in the case of concentration.

An increase in thermophoresis parameter Nt generates movement in the nanoparticles from the higher temperature region to the lower in the boundary layer region. Thus increases in

Nt implies an increase in both the temperature and concentration profiles as shown in Fig. 11(a) and Fig. 11(b). The advancement of temperature with the Biot number Bi is illustrated in Fig. 12. This is due to the fact that convective heating as well as temperature gradient increases with Bi .

The influence of the Lewis number Le on the concentration profile is illustrated in Figure 13. It can be observed that increase in Le reduces the concentration boundary layer.

Tables 1, 2 and 3 exhibit excellent correlation between the present and the previous results under limiting conditions.

The influence of various parameters such as $\delta, R, Nb, Nt, Ec, Bi$ and γ on skin friction coefficient, Nusselt number and Sherwood number are shown in Table 4. From the table, it is seen that skin friction coefficient enhances with δ . Nusselt number and Sherwood number enhance with R and the reverse trend is observed with δ and Nt . Nusselt number declines and Sherwood number rises with Nb, Ec, γ .

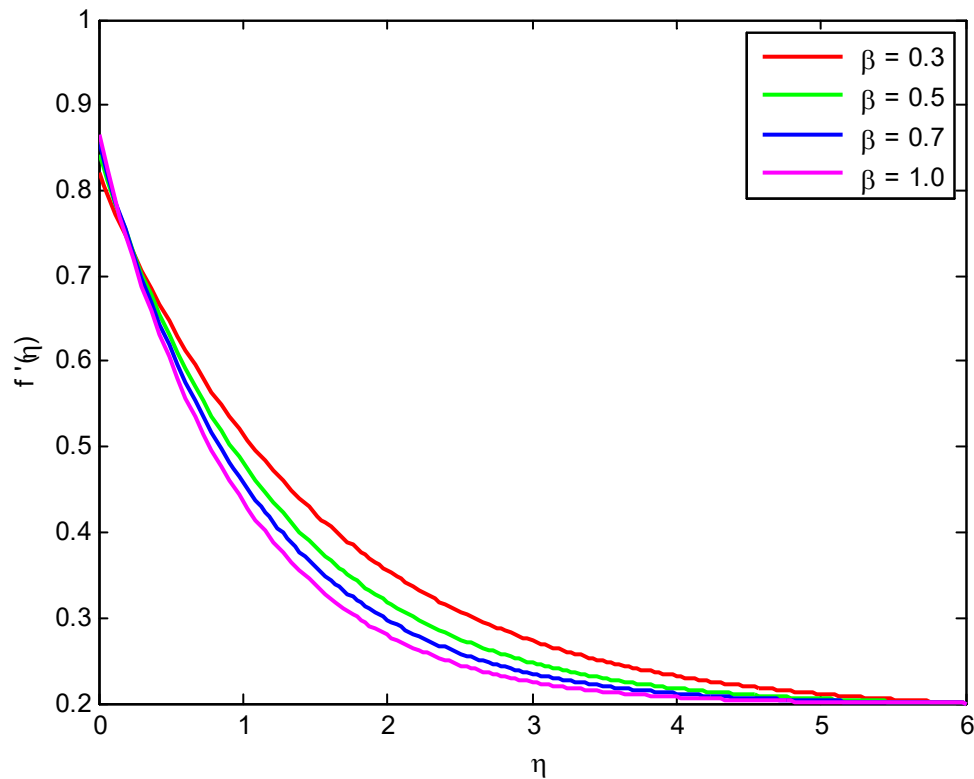


Fig. 1(a). Velocity profiles for various values of β

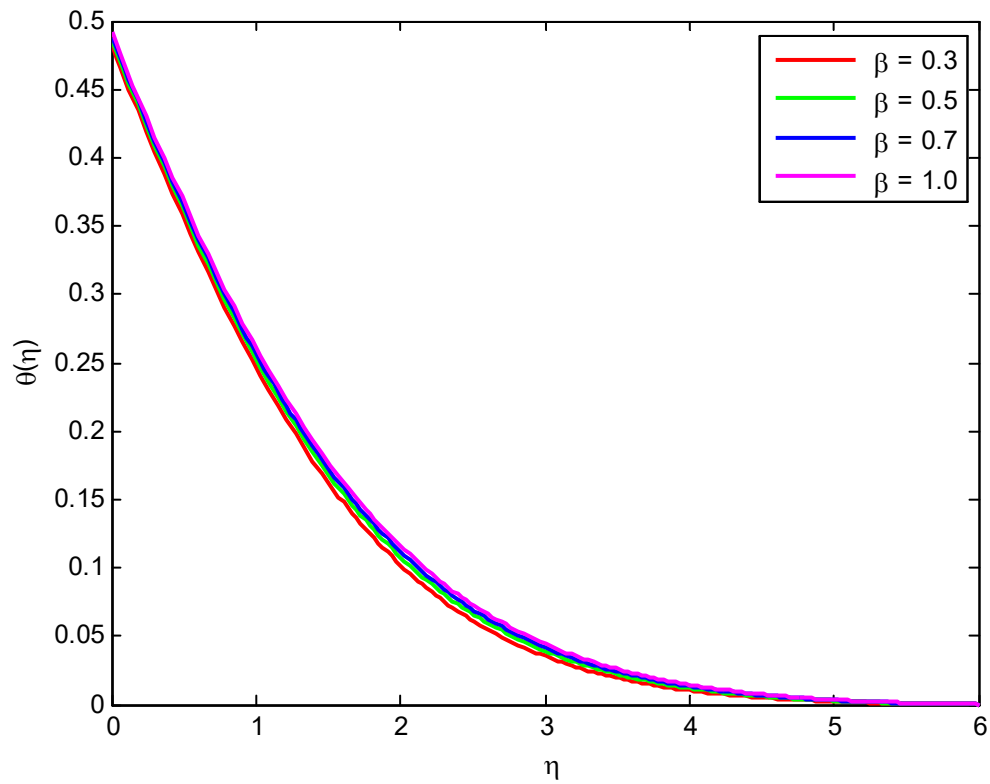


Fig.1(b). Temperature profiles for various values of β

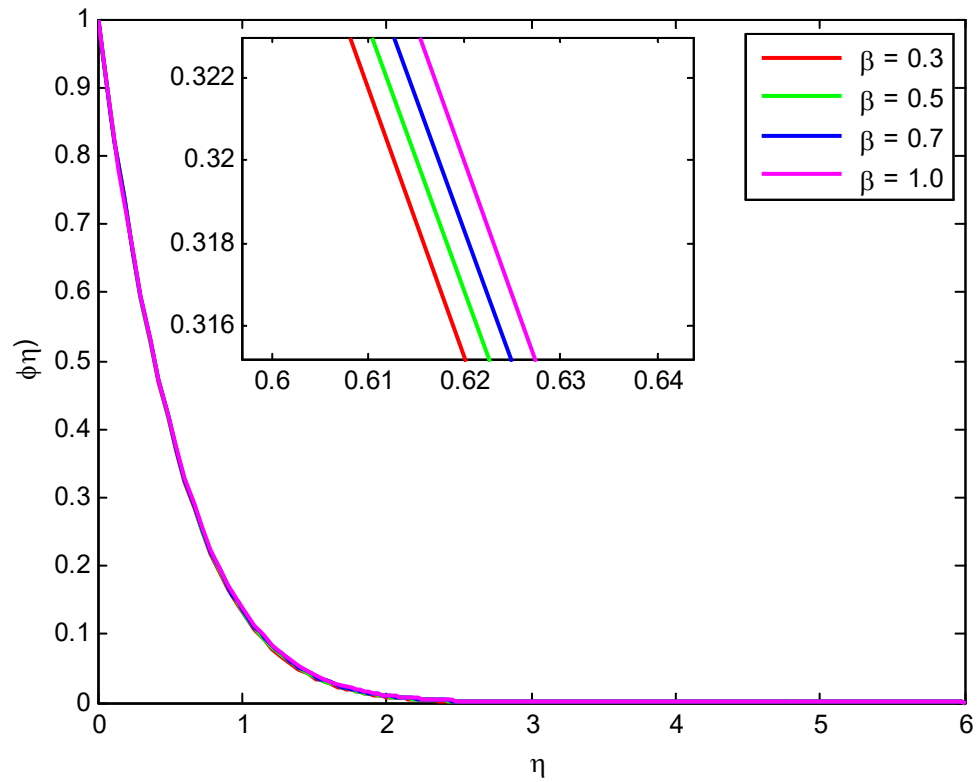


Fig. 1(c). Concentration profiles for various values of β

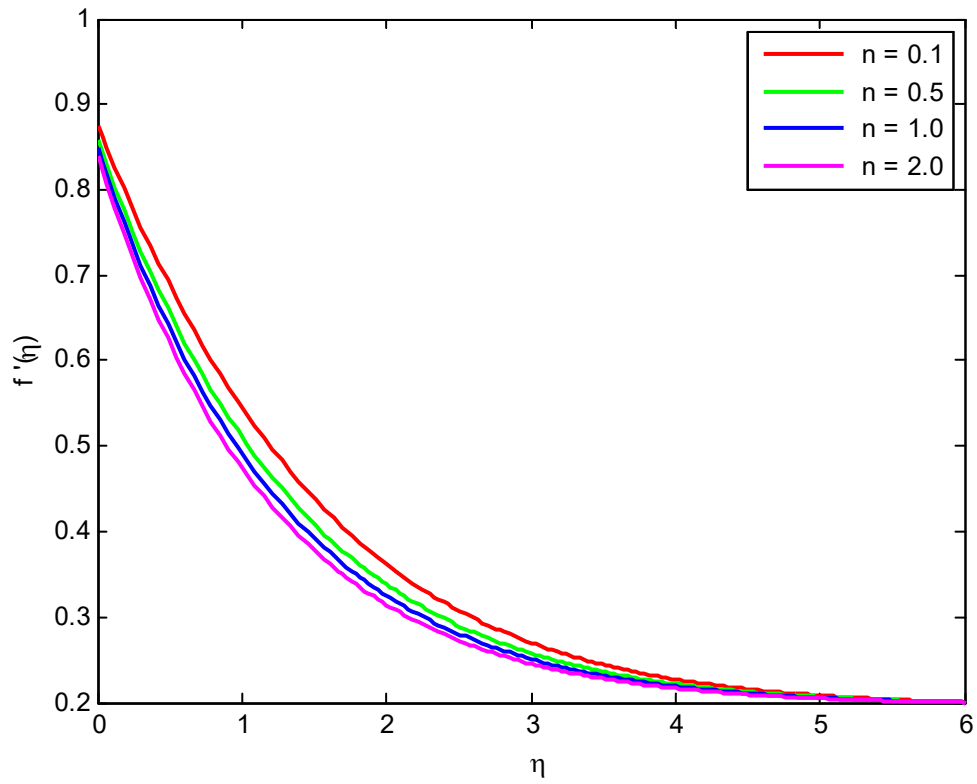


Fig.2 (a). Velocity profiles for various values of n

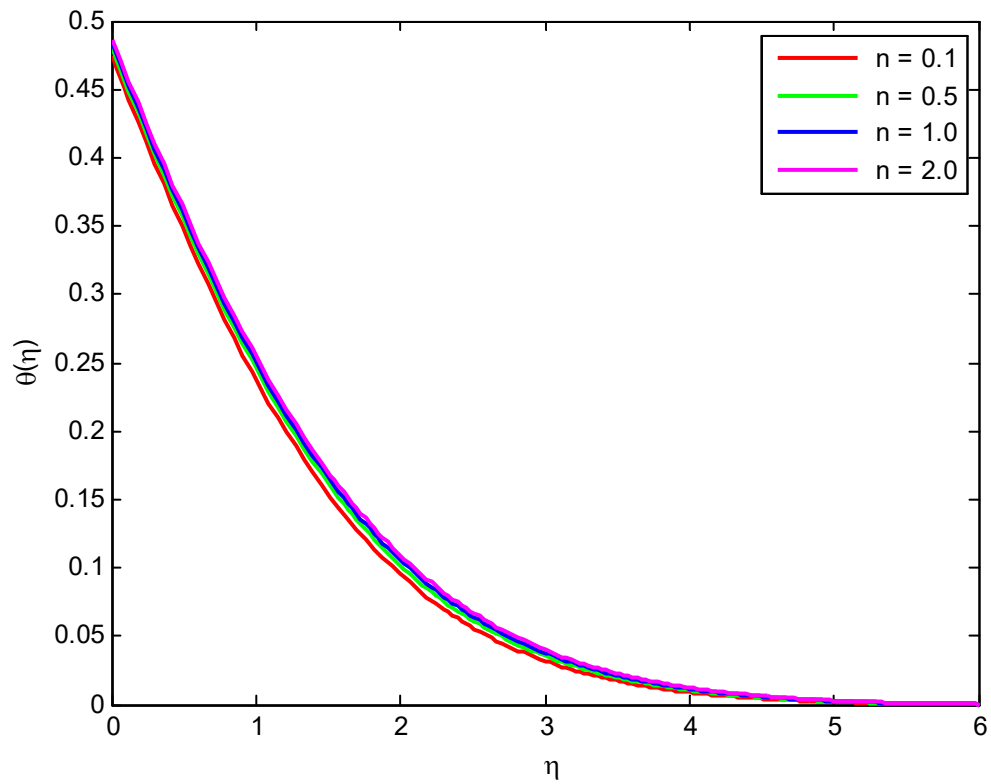


Fig. 2(b). Temperature profiles for various values of n

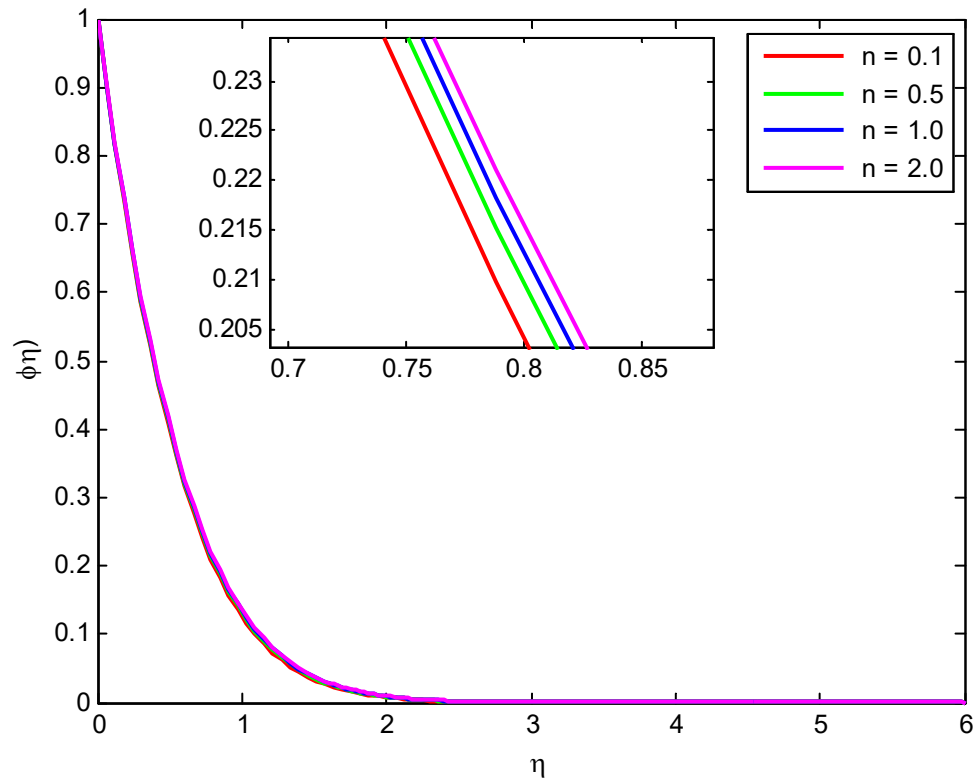


Fig. 2(c). Concentration profiles for various values of n

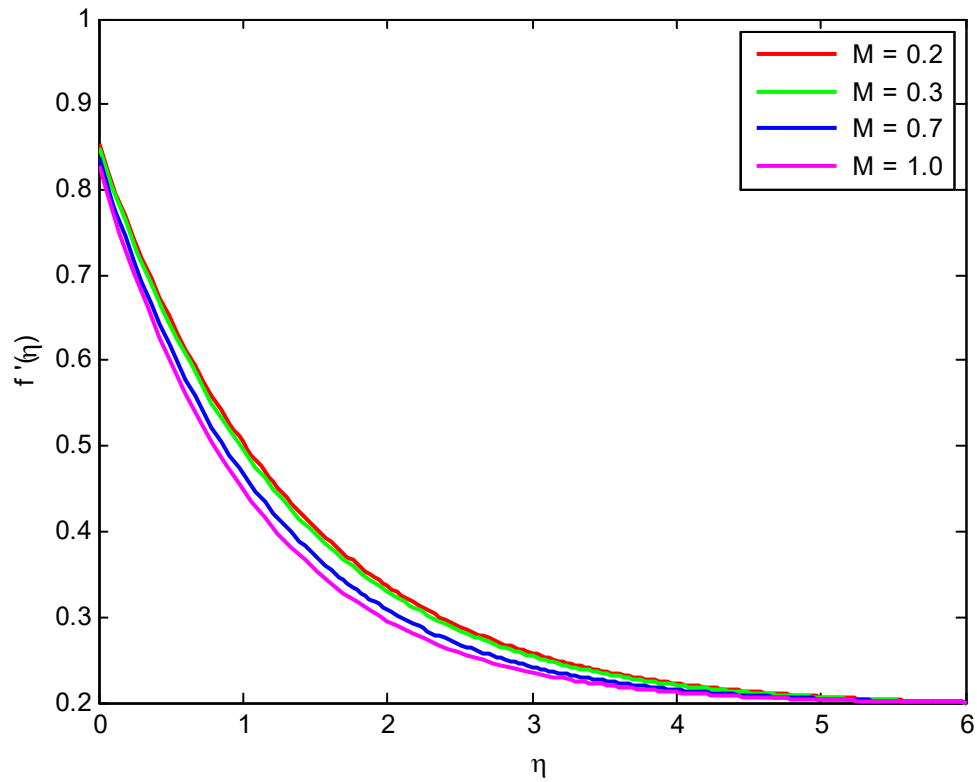


Fig.3. Velocity profiles for various values of M

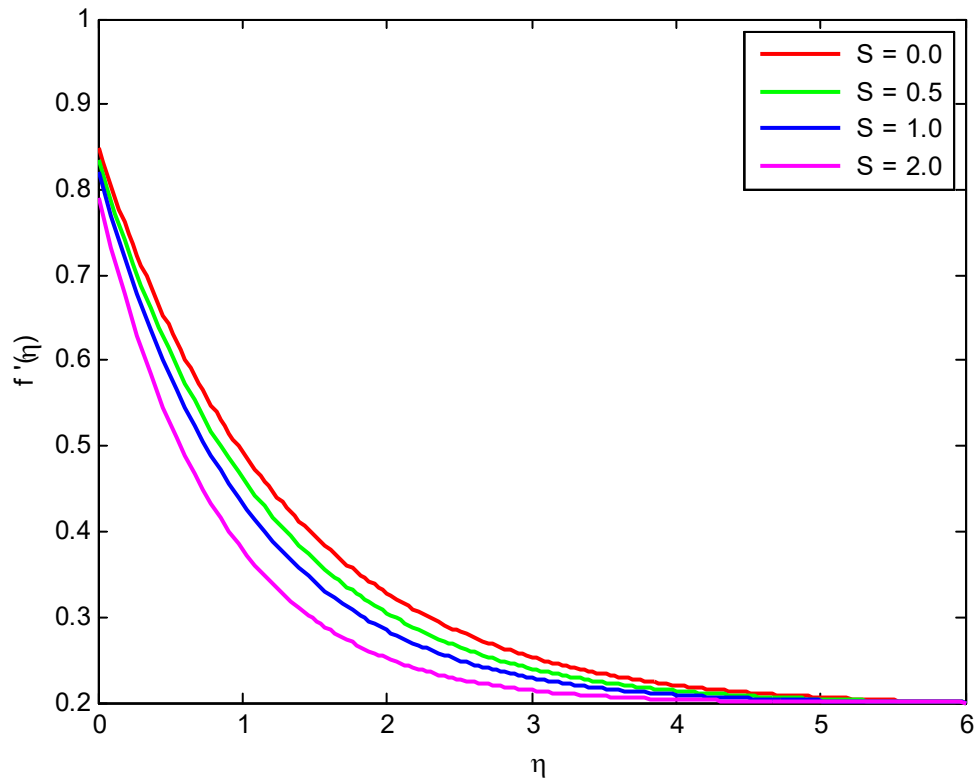


Fig.4. Velocity profiles for various values of S

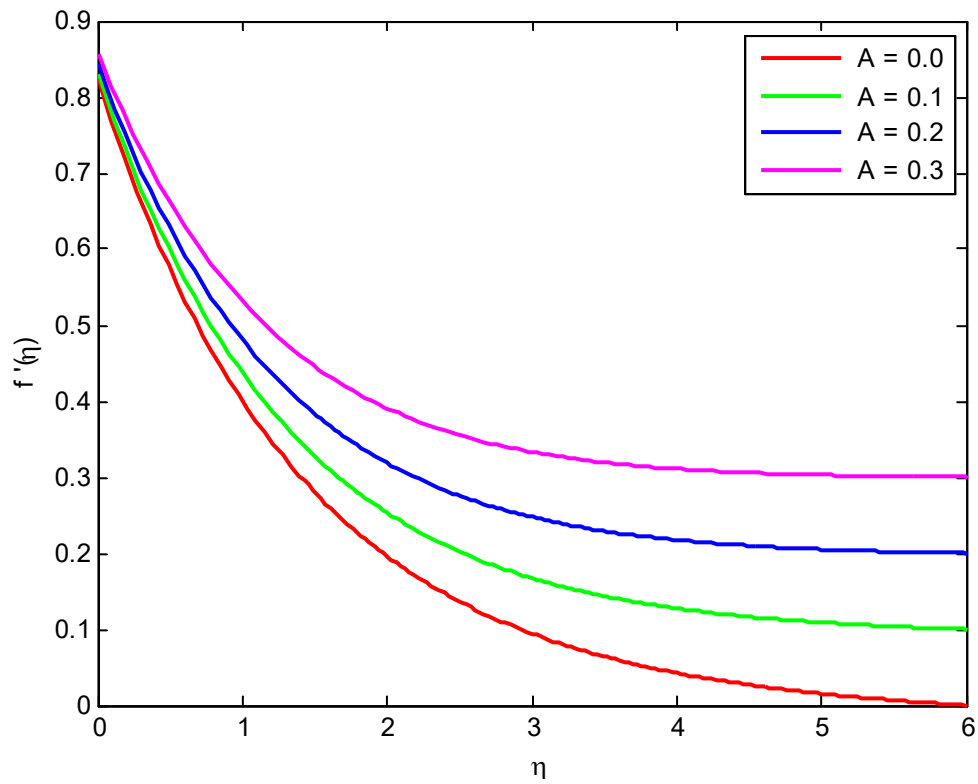


Fig.5. Velocity profiles for various values of A

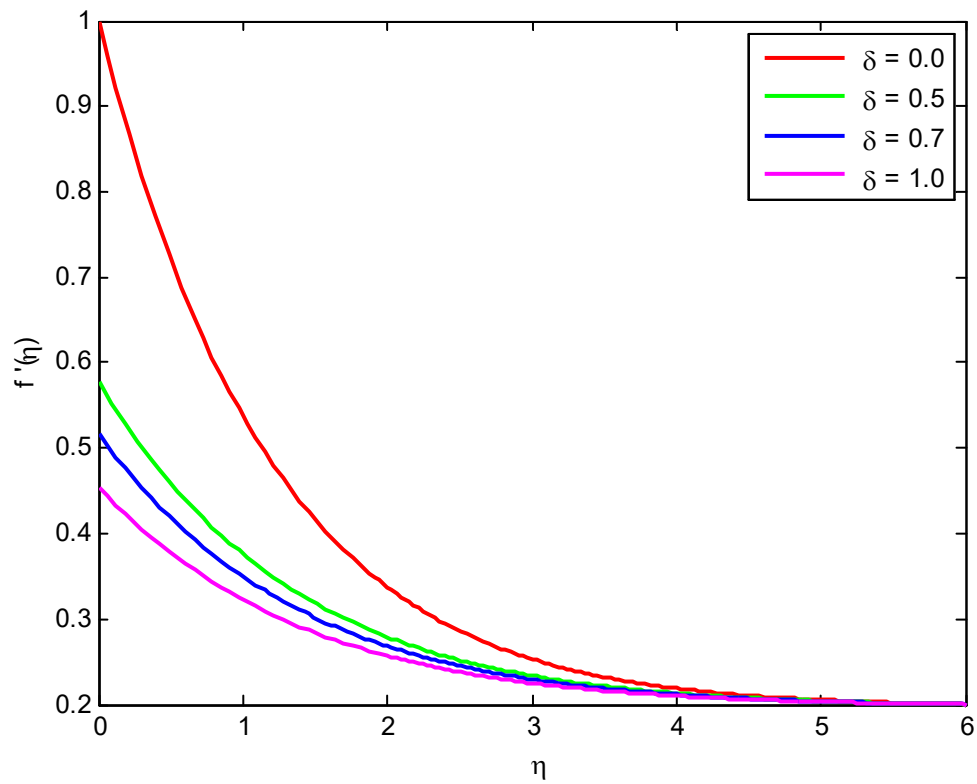


Fig.6. Velocity profiles for various values of δ

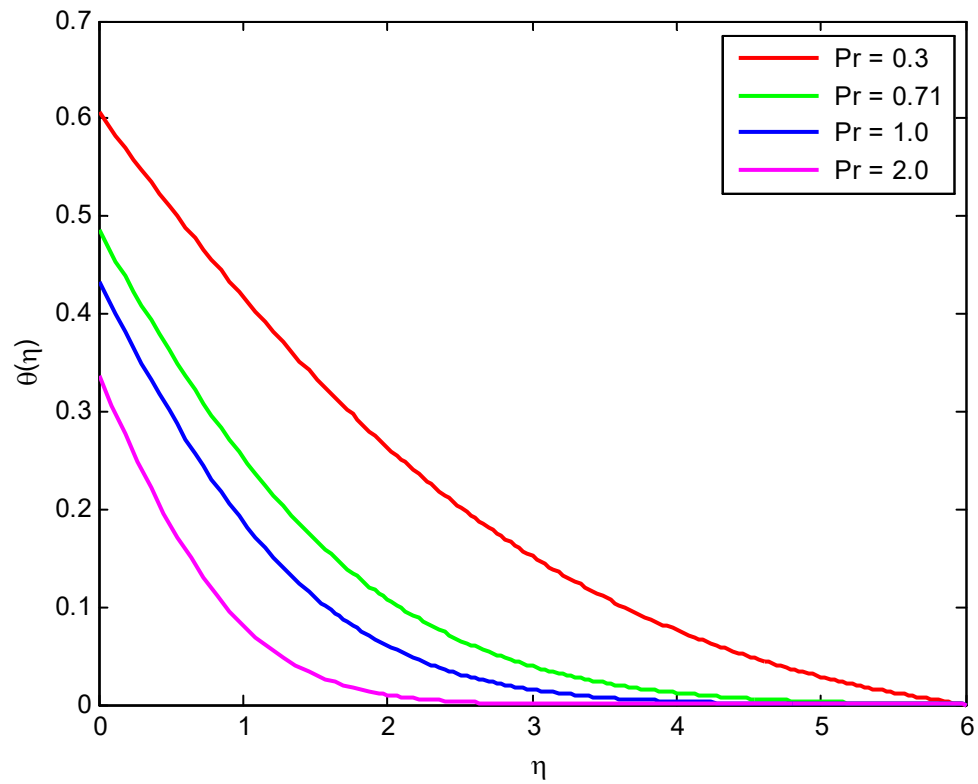


Fig. 7. Temperature profiles for various values of Pr

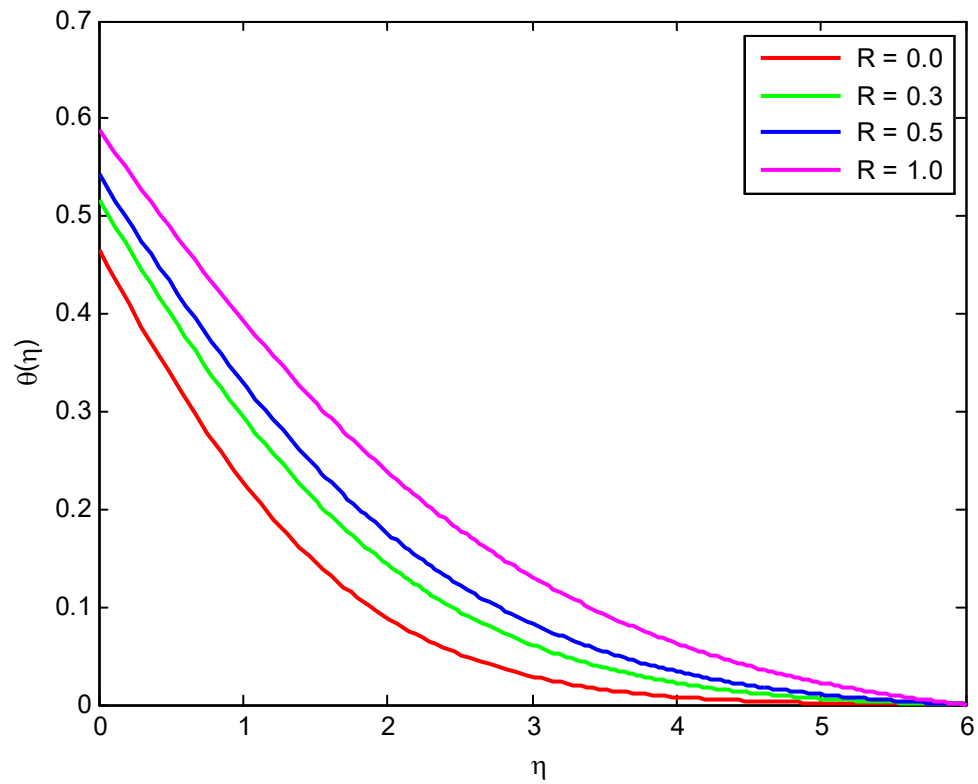


Fig. 8. Temperature profiles for various values of R

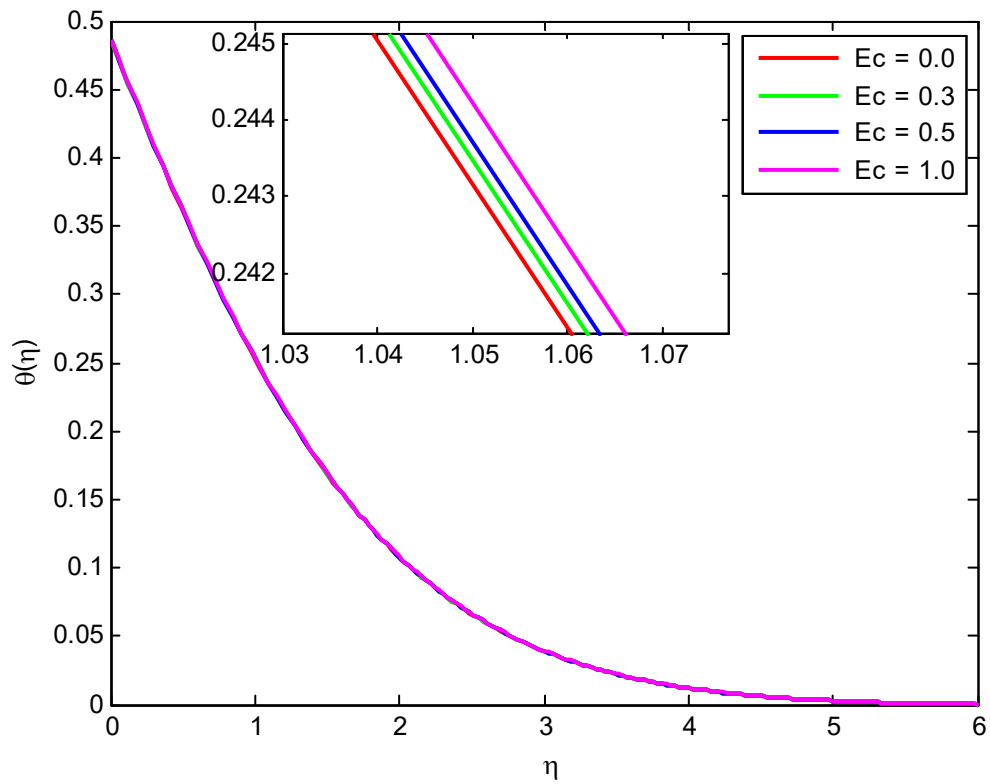


Fig. 9. Temperature profiles for various values of Ec

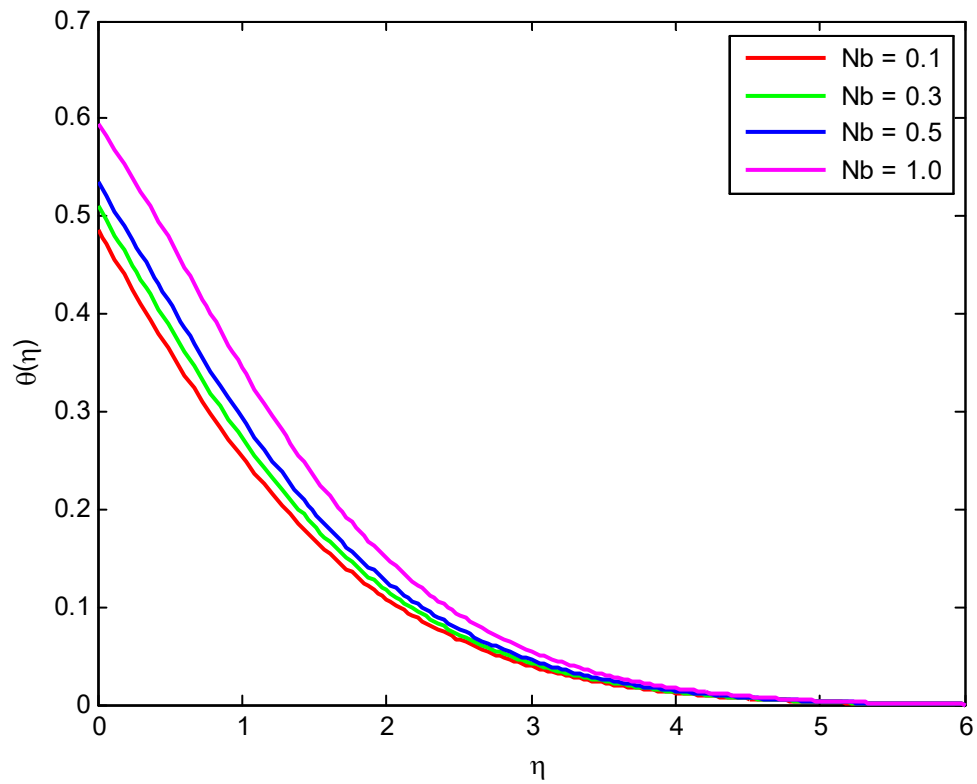


Fig. 10(a). Temperature profiles for various values of Nb

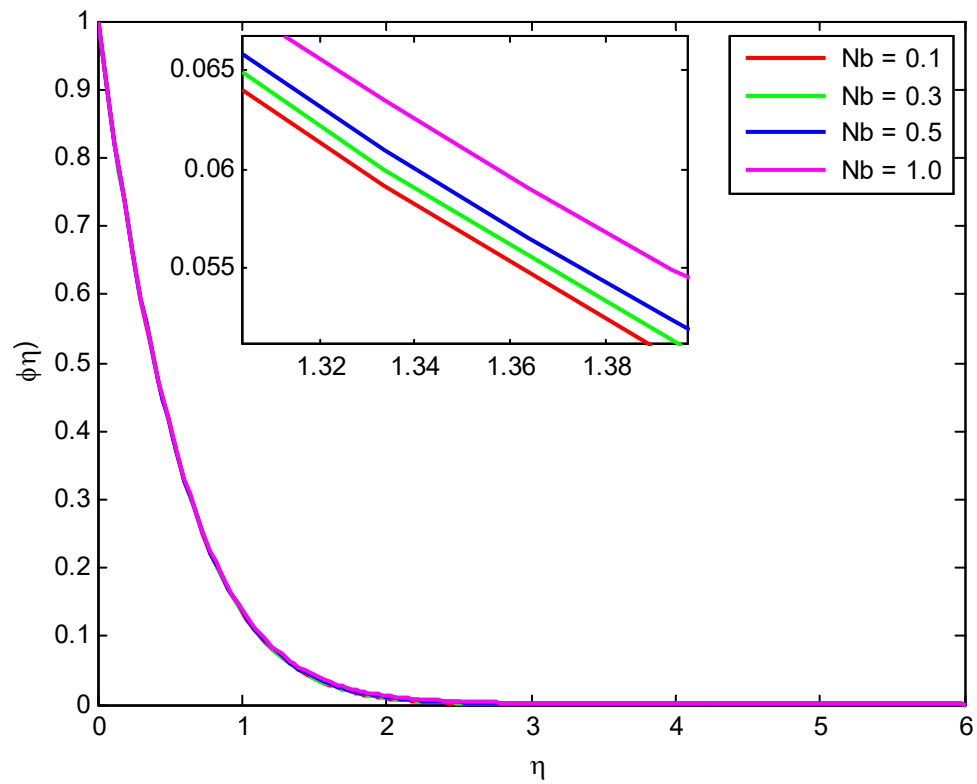


Fig. 10 (b). Concentration profiles for various values of Nb

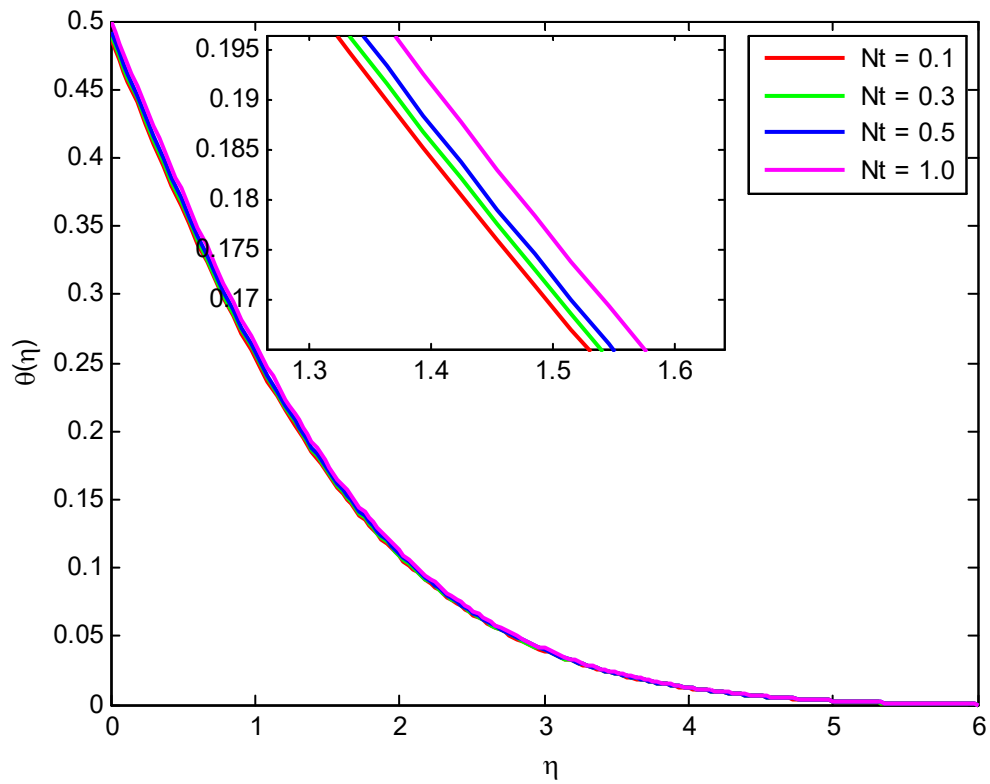


Fig. 11(a). Temperature profiles for various vales of Nt

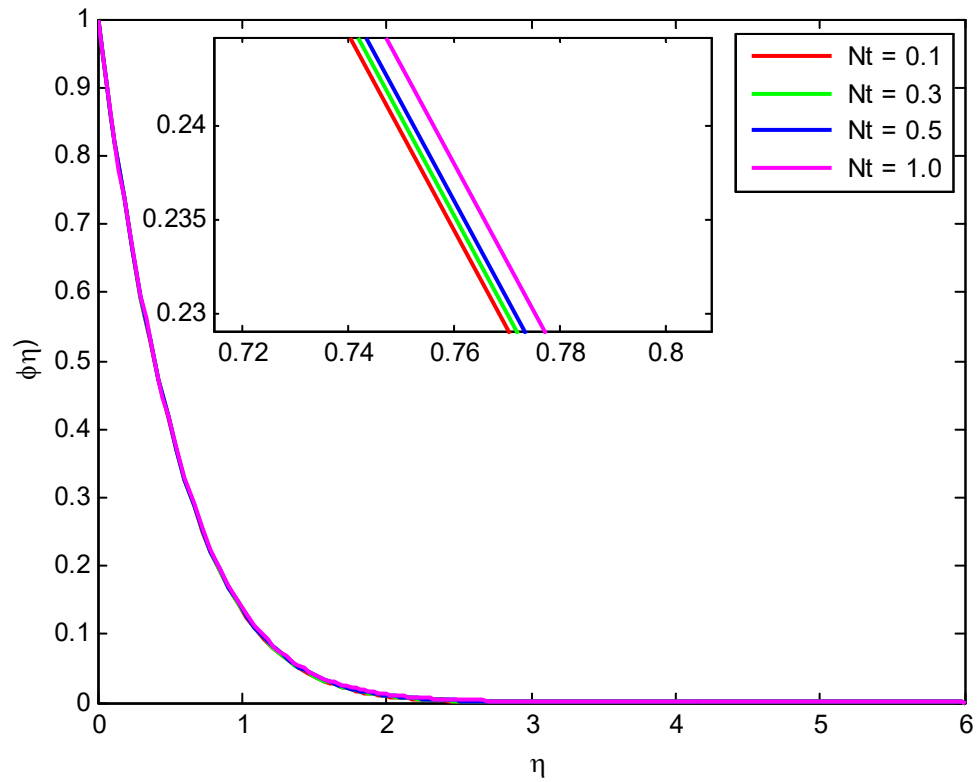


Fig. 11(b). Concentration profiles for various values of Nt

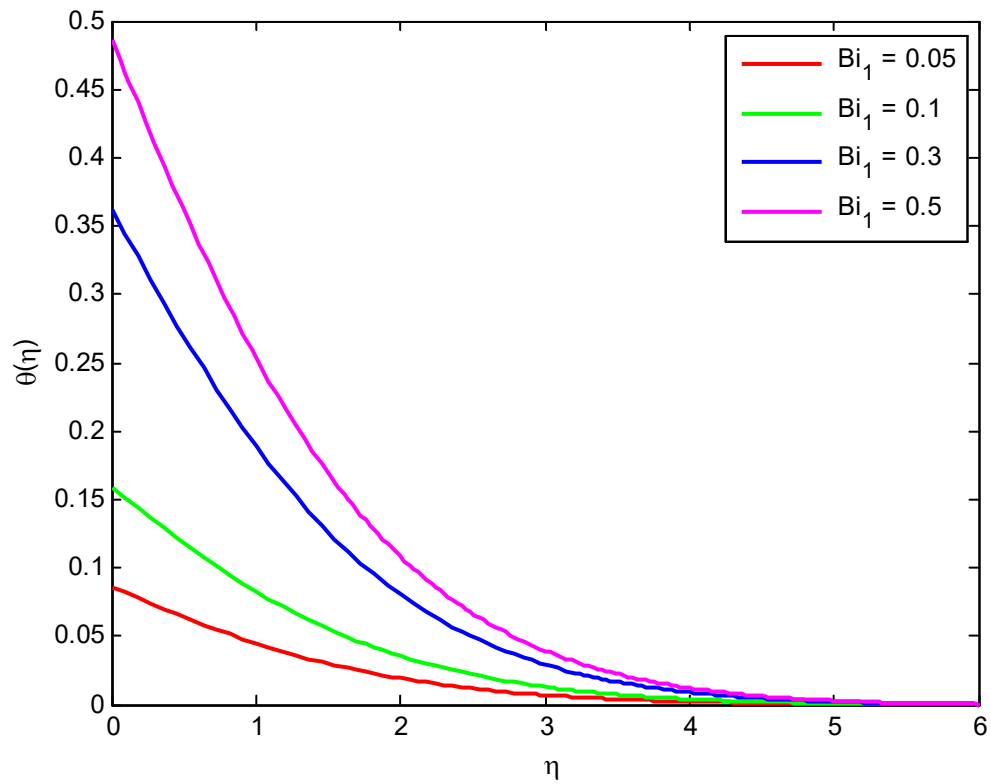


Fig. 12. Temperature profiles for various values of Bi_1

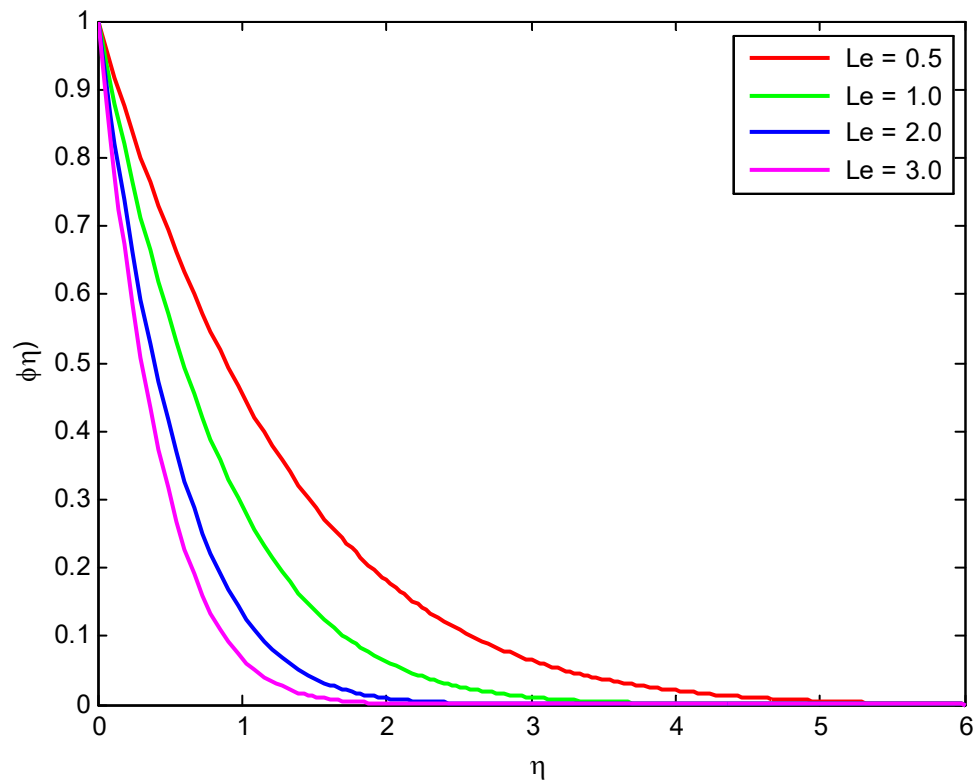


Fig. 13. Concentration profiles for various values of Le

Table 1. Comparison of skin friction coefficient for different values of β and A when $M = 0, \delta = 0.0, S = 0.0$ and $n = 1.0$.

| β | A | Mondal et al. [35] | Present |
|---------|------|--------------------|----------|
| 1 | 0.0 | -1.41421 | -1.41421 |
| 5 | 0.0 | -1.09544 | -1.09545 |
| 1000 | 0.01 | -0.99782 | -0.99801 |
| 1000 | 0.1 | -0.96937 | -0.96937 |
| 1000 | 0.2 | -0.91811 | -0.91811 |

Table 2. Comparison of $-f''(0)$ for different values of δ when

$M = 0, A = 0.0, \beta = 1000, S = 0.0$ and $n = 1.0$.

| δ | Ibrahim and Makinde [16] | Oyelakin et al. [35] | Present |
|----------|--------------------------|----------------------|---------|
| 0.0 | 1.0000 | 1.000000 | 1.00000 |
| 0.1 | 0.8721 | 0.872083 | 0.87208 |
| 0.2 | 0.7764 | 0.776377 | 0.77638 |
| 0.5 | 0.5912 | 0.591195 | 0.59121 |
| 1.0 | -- | 0.430160 | 0.43017 |
| 2.0 | 0.2840 | 0.283979 | 0.28397 |
| 3.0 | -- | 0.214054 | 0.21406 |
| 5.0 | 0.1448 | 0.144714 | 0.14484 |
| 10.0 | 0.0812 | 0.080932 | 0.08125 |

Table 3. Comparison of $-\theta'(0)$ and $-\phi'(0)$ when

$M = A = \delta = S = R = Ec = Q = \gamma = 0.0, Nb = 0.5, Bi = 10000, Pr = Le = 2.0$ and $\beta \rightarrow \infty$.

| n | Nt | Rana and Bhargava [36] | | Mabood and Khan [37] | | Present | |
|-----|------|------------------------|-------------|----------------------|-------------|---------------|-------------|
| | | $-\theta'(0)$ | $-\phi'(0)$ | $-\theta'(0)$ | $-\phi'(0)$ | $-\theta'(0)$ | $-\phi'(0)$ |
| 0.2 | 0.3 | 0.4533 | 0.8395 | 0.4520 | 0.8402 | 0.45197 | 0.84011 |
| | 0.5 | 0.3999 | 0.8048 | 0.3987 | 0.8059 | 0.39905 | 0.80571 |
| 3.0 | 0.3 | 0.4282 | 0.7785 | 0.4271 | 0.7791 | 0.42725 | 0.77919 |
| | 0.5 | 0.3786 | 0.8323 | 0.3775 | 0.7390 | 0.37772 | 0.73878 |
| 10 | 0.3 | 0.4277 | 0.7654 | 0.4216 | 0.7660 | 0.42180 | 0.76598 |
| | 0.5 | 0.3739 | 0.7238 | 0.3728 | 0.7248 | 0.37309 | 0.72436 |

Table 4. Numerical values of skin friction coefficient $-\left(1 + \frac{1}{\beta}\right)f''(0)$, Nusselt number

$-\left(1 + \frac{4}{3}R\right)\theta'(0)$ and Sherwood number $-\phi'(0)$ for different values of $\delta, R, Nb, Nt, Ec, Q, Bi, \gamma$.

| δ | R | Nb | Nt | Ec | Q | Bi | γ | $-\left(1 + \frac{1}{\beta}\right)f''(0)$ | $-\left(1 + \frac{4}{3}R\right)\theta'(0)$ | $-\phi'(0)$ |
|----------|-----|------|------|------|------|------|----------|---|--|-------------|
| 0.1 | 0.1 | 0.2 | 0.2 | 0.1 | 0.1 | 0.5 | 0.2 | -1.69743 | 0.33294 | 0.77274 |
| 0.5 | | | | | | | | -0.95332 | 0.33197 | 0.72178 |
| 1.0 | | | | | | | | -0.61221 | 0.32883 | 0.69758 |
| | 0.5 | | | | | | | -- | 0.42884 | 0.81317 |
| | 0.7 | | | | | | | -- | 0.46962 | 0.82831 |
| | | 0.5 | | | | | | -- | 0.31795 | 0.90492 |
| | | 1.0 | | | | | | -- | 0.29130 | 0.94929 |
| | | | 0.3 | | | | | -- | 0.33174 | 0.67008 |
| | | | 0.5 | | | | | -- | 0.32929 | 0.46868 |
| | | | | 0.5 | | | | -- | 0.27542 | 0.83879 |
| | | | | 1.0 | | | | -- | 0.20317 | 0.92169 |
| | | | | | -0.2 | | | -- | 0.35715 | 0.74643 |
| | | | | | 0.0 | | | -- | 0.34220 | 0.76274 |
| | | | | | | 0.1 | | -- | 0.09665 | 0.92602 |
| | | | | | | 2.0 | | -- | 0.60994 | 0.59416 |
| | | | | | | | 0.0 | -- | 0.33348 | 0.65631 |
| | | | | | | | 0.5 | -- | 0.33233 | 0.91960 |

References

1. S. U. S. Choi, Enhancing thermal conductivity of fluids with nanoparticles, *The Proceedings of the 1995 ASME International Mechanical Engineering Congress and Exposition, San Francisco, CA, ASME, FED*, 231, 99-105, 1995.
2. J. Buongiorno, Convective transport in nanofluids, *Journal of Heat Transfer*, 128, 240-250, 2006.
3. W. A. Khan and I. Pop, Boundary-layer flow of a nanofluid past a stretching sheet, *International Journal of Heat and Mass Transfer*, 53, 2477-2483, 2010.
4. M. Mustafa, T. Hayat, I. Pop, S. Asghar and S. Obaidat, Stagnation-point flow of a nanofluid towards a stretching sheet, *International Journal of Heat and Mass Transfer*, 54, 5588-5594, 2011.
5. W. Ibrahim, B. Shankar and M. M. Nandeppanavar, MHD stagnation point flow and heat transfer due to nanofluid towards a stretching sheet, *International Journal of Heat and Mass Transfer*, 56, 1-9, 2013.
6. N. Bachok, A. Ishak and I. Pop, Stagnation-point flow over a stretching/shrinking sheet in a nanofluid, *Nanoscale Research Letters*, 6, 1-10, 2013.
7. N. A. Yacob, A. Ishak, I. Pop and K. Vajavelu, Boundary layer flow past a stretching/shrinking surface beneath an external uniform shear flow with a convective surface boundary condition in a nanofluid, *Nanoscale Research Letters*, 6, 1-7, 2011.
8. O. D. Makinde and A. Aziz, Boundary layer flow of a nanofluid past a stretching sheet with a convective boundary conditions, *International Journal of Thermal Sciences*, 50, 1326-1332, 2011.
9. M. Gnaneswara Reddy, *Int. J. Heat and Technology* 32, 1 (2014).
10. M. Gnaneswara Reddy, P. Padma, B. Shankar, and B. J. Gireesha, *J. Nanofluids* 5, 753 (2016).
11. P. Sathies Kumar and K. Gangadhar., Effect of chemical reaction on slip flow of MHD Casson fluid over a stretching sheet with heat and mass transfer, *Advances in Applied Science Research*, 2015, 6(8):205-223.
12. K. Bhattacharyya, MHD stagnation point flow of Casson fluid and heat transfer over a stretching sheet with thermal radiation, *Journal of Thermodynamics*, Volume 2013 (2013), Article ID 169674, 9 pages.

13. Benazir J., Sivaraj A, Makinde OD. Unsteady magnetohydrodynamic Casson fluid flow over a vertical cone and flat plate with non-uniform heat source/sink. *Int J Eng Res Africa*. 2016;21: 69–83.
14. Nadeem S, Haq RU, Akbar NS, Khan ZH. MHD three-dimensional Casson fluid flow past a porous linearly stretching sheet. *Alexandria Eng J. Faculty of Engineering, Alexandria University*; 2013;52: 577–582. doi: 10.1016/j.aej.2013.08.005.
15. U.H. Rizwan, S. Nadeem, Z.H. Khan, T.G. Okedayo, Convective heat transfer and MHD effects on Casson nanofluid flow over a shrinking sheet, *Cent. Eur. J. Phys*, 12 (12) (2014), pp. 862–871.
16. W. Ibrahim and O. D. Makinde, Magnetohydrodynamic stagnation point flow and heat transfer of Casson nanofluid past a stretching sheet with slip and convective boundary conditions, *Journal of Aerospace Engineering*, 29, 1-11, 2016. (Base Paper)
17. S. A. Shehzad, T. Hayat, M. Qasim and S. Asghar, Effects of mass transfer on MHD flow of Casson fluid with chemical reaction and suction, *Brazilian journal of chemical engineering*, 30 (1), 187-195 (2013).
18. Mukhopadhyay S. Effects of thermal radiation on Casson fluid flow and heat transfer over an unsteady stretching surface subjected to suction/blowing. *Chinese Phys B*. 2013;22: 114702. doi: 10.1088/1674-1056/22/11/114702.
19. I. S. Oyelakin, S. Mondal and P. Sibanda, Unsteady Casson nanofluid flow over a stretching sheet with thermal radiation, convective and slip boundary conditions, *Alexandria Engineering Journal*, 55, 1025-1035, 2016.
20. Mukhopadhyay, S., Casson fluid flow and heat transfer over a nonlinearly stretching surface, *Chin. Phys. B*, 22 (2013), 7, pp. 074701, DOI: 10.1088/1674-1056/22/7/074701
21. Vajravelu, K. (2001) Viscous Flow over a Nonlinearly Stretching Sheet. *Applied Mathematics and Computation*, 124, 281-288
22. Cortell, R. (2007) Viscous Flow and Heat Transfer over a Nonlinearly Stretching Sheet. *Applied Mathematics and Computation*, 184, 864-873. <http://dx.doi.org/10.1016/j.amc.2006.06.077>
23. D Pal., N Roy., K Vajravelu, Effects of thermal radiation and Ohmic dissipation on MHD Casson nanofluid flow over a vertical non-linear stretching surface using scaling group, *International Journal of Mechanical Sciences* 114 (2016) 257–267.
24. Ullah I, Bhattacharyya K, Shafie S, Khan I (2016) Unsteady MHD Mixed Convection Slip Flow of Casson Fluid over Nonlinearly Stretching Sheet Embedded in a Porous Medium with Chemical Reaction, Thermal Radiation, Heat Generation/Absorption and Convective Boundary Conditions. *PLoS ONE* 11(10): e0165348. doi:10.1371/journal.pone.0165348

25. T. Hayat, M. Bilal Ashraf, S. A. Shehzad and A. Alsaedi, Mixed Convection Flow of Casson Nanofluid over a Stretching Sheet with Convectively Heated Chemical Reaction and Heat Source/Sink, *Journal of Applied Fluid Mechanics*, Vol. 8, No. 4, pp. 803-813, 2015.
26. Ziabakhsh, Z., Domairry, G., Bararnia, H. and Babazadeh, H., Analytical solution of flow and diffusion of chemically reactive species over a nonlinearly stretching sheet immersed in a porous medium. *J. Taiwan Institute Chemical Eng.*, 41, p. 22 (2010).
27. Abbas, Z. and Hayat, T. (2011) Stagnation Slip Flow and Heat Transfer over a Nonlinear Stretching Sheet. *Numerical Methods for Partial Differential Equations*, 27, 302-314.
28. Hayat, T., Javed, T. and Abbas, Z. (2009) MHD Flow of a Micropolar Fluid near a Stagnation-Point Towards a Non-Linear Stretching Surface. *Nonlinear Analysis: Real World Applications*, 10, 1514-1526
29. M. Gnaneswara Reddy, *Journal of Engineering Physics and Thermophysics* 88, 240 (2015).
30. Mabood, F., Khan, W.A. and Ismail, A.I.M. (2015) MHD Boundary Layer Flow and Heat Transfer of Nanofluids over a Nonlinear Stretching Sheet: A Numerical Study. *Journal of Magnetism and Magnetic Materials*, 374, 569-576.
31. Prasad, K.V., Vajravelu, K. and Dattri, P.S. (2010) Mixed Convection Heat Transfer over a Non-Linear Stretching surface with Variable Fluid Properties. *International Journal of Non-Linear Mechanics*, 45, 320-330. <http://dx.doi.org/10.1016/j.ijnonlinmec.2009.12.003>
32. Rana, P. and Bhargava, R. (2012) Flow and Heat Transfer of a Nanofluid over a Nonlinearly Stretching Sheet: A Numerical Study. *Communications in Nonlinear Science and Numerical Simulation*, 17, 212-226. <http://dx.doi.org/10.1016/j.cnsns.2011.05.009>
33. Ghotbi, A.R. (2009) Homotopy Analysis Method for Solving the MHD flow over a Non-Linear Stretching Sheet. *Communications in Nonlinear Science and Numerical Simulation*, 14, 2653-2663. <http://dx.doi.org/10.1016/j.cnsns.2008.08.006>
34. Fanga, T. (2014) Magneto-Hydrodynamic Viscous Flow over a Nonlinearly Moving Surface: Closed-Form Solutions. *The European Physical Journal Plus*, 129, 92. <http://dx.doi.org/10.1140/epjp/i2014-14092-4>.
35. I. S. Oyelakin, S. Mondal and P. Sibanda, Unsteady Casson nanofluid flow over a stretching sheet with thermal radiation, convective and slip boundary conditions, *Alexandria Engineering Journal*, 55, 1025-1035, 2016.

36. P. Rana and R. Bhargava, Flow and heat transfer of a nanofluid over a nonlinearly stretching sheet: A numerical study, *Communications in Nonlinear Science and Numerical Simulation*, 17, 212-226, 2012.
37. F. Mabood, W. A. Khan and A. I. M. Ismail, MHD boundary layer flow and heat transfer of nanofluids over a nonlinear stretching sheet: A numerical study, *Journal of Magnetism and Magnetic Materials*, 374, 569-576, 2015.